

평면 경사자계 코일을 사용한 고분해능  
NMR 생체 영상법에 관한 연구

이정환, 오우진, 조장희  
한국과학기술원 전기및 전자공학과

*In Vivo* High Resolution NMR Imaging by Using  
Surface Gradient Coil

Yi Jeong-Han, Oh Woo-Jin and Cho Zang-Hee  
Dept. of E.E., KAIST

**Abstract**

A new *in vivo* high resolution imaging method which is performed with a newly developed three channel surface gradient coil (SGC) is described. The surface gradient coil can produce more than an order of magnitude stronger gradient fields with good linearity within a limited imaging region. To increase the signal to noise ratio (SNR), we have developed an RF coil integrated surface gradient coil set. In this paper, the geometrical structures and characteristics of the proposed surface gradient coil are discussed and experimentally obtained high resolution images (50  $\mu\text{m}$  to 100  $\mu\text{m}$ ) of a water filled phantom and a human volunteer's knee using the new surface RF coil integrated SGC set are presented for the demonstration of the *in vivo* high resolution imaging capability of the new imaging method.

**Introduction**

Since the development of NMR imaging there have been a lot of investigations on the high resolution NMR imaging such as the NMR microscopy (1-4). Although it is considered as a difficult task, the high resolution *in vivo* human body imaging has several interesting features such as the fine anatomical details and pathological structures of bone joints, eye ball and optic nerves (5) that would normally not be seen by conventional imaging. In general, high resolution imaging requires the use of strong gradient fields since high spatial resolution requires proportionally strong gradient fields as well as high sensitivity RF coil to compensate for the loss of signal to noise ratio (SNR) due to the reduced voxel size (6,7). Another requirement for high resolution imaging of a large object (i.e., human body) is localization so that one can reduce the size of the imaging matrix as well as the image reconstruction time. Although there have been attempts to improve the resolution down to 100  $\mu\text{m}$  or less especially for small animals and various excised objects, it is generally difficult to increase the

gradient field strength beyond a certain limit for an object of a large size such as human body. In this paper we discuss a new surface gradient coil system of planar form which is suitable for *in vivo* high resolution imaging of a human body (8). In the proposed surface gradient coil, we have also integrated a surface RF coil onto the SGC to develop a set of imaging probe. This SGC set improves the sensitivity for localized region in the *in vivo* high resolution imaging of the human body.

**Method**

Geometries of the three channel surface gradient coils of  $G_x$ ,  $G_y$  and  $G_z$  are shown in Figs.1(a), (b) and (c). The surface Gradient coil is a new concept of gradient coil, which constructed on a flat plate while the conventional gradient coil is constructed on a cylinder (7,9). Figs.2(b), (c) and (d) are computer simulations of grid phantom (a). Fig.4(b) is a image of a parallel plane of  $y = 0.5W$  while Figs.2(c) and (d) depict the gradient field variations which affect the image resolution along the  $y$ -direction (depth) when the planes are perpendicular to the SGC. While images along the perpendicular planes are gradually shrunken along the  $y$ -direction, large portions of the parallel plane images relative to the surface gradient coil width ( $W$ ) remain linear. These characteristics are key points of SGC.

The unique characteristic of the surface gradient coil is the localized strong gradient fields, which makes possible parallel plane imaging along the depth direction ( $y$ -direction in this case). The localized strong gradient fields, therefore, allow high resolution imaging which is free of aliasing (or folding) effect especially in the direction of the phase encoding. Another advantage of the SGC (surface gradient coil) is the possibility of integrating a surface RF coil, thereby forming a SGC set or probe. This combination provides unique feature such as the movability and the development of a planar structure NMR imaging probe

with maximized sensitivity. In fact, the SGC set or probe satisfies the basic requirements of high resolution imaging for clinical settings (i.e., human imaging), namely, the availability of strong gradient fields with spatial localization characteristics by the SGC and the high sensitivity by the surface RF coil. Fig.3 illustrates the movability of the SGC NMR probe. The SGC set which is a combination of the SGC and the surface RF coil can be positioned onto any desired parts of the body to perform imaging.

A set of the proposed three channel surface gradient coils was constructed on a 12.5cm x 25cm acrylic plate (see Fig.5 ). The gradient strengths of x-, y- and z-SGC are 6 G/cm ~ 25 G/cm, 7 G/cm ~ 28 G/cm and 15 G/cm ~ 53 G/cm with 100 amperes of driving currents within a 5cm x 5cm x 5cm region, respectively. As it is seen, gradient strengths obtained are much larger than the fields that can be obtained from the conventional whole-body MRI system where a maximum of 0.5 ~ 1 G/cm is commonly recorded. For example, for 100 $\mu$ m resolution of H<sup>1</sup> imaging with T<sub>acq</sub> = 5.12 msec, the required readout gradient strength is 4.6G/cm and is much larger than the gradient strength that can be obtained from the conventional whole-body gradient coil. As it will be shown, a number of high resolution images were obtained using the new SGC set (surface RF coil integrated).

A pulse sequence used for higher resolution imaging using the SGC in combination with the localized imaging method is shown in Fig.4(a) and its corresponding imaging geometry is shown in Fig.4(b). The following is a brief explanation of the pulse sequence: First, a thin slice is selected by the selective 90° RF pulse in conjunction with G<sub>S</sub> gradient (i.e., G<sub>y</sub>) followed by the phase encoding G<sub>SC</sub> (i.e., G<sub>x</sub>) with a selective 180° RF pulse which will restrict the region in the z-direction, thereby, preventing aliasing. Finally the readout gradient G<sub>r</sub> ( i.e., G<sub>z</sub> ) is added to readout the signal. Readout directional aliasing is prevented by the low pass filter ( LPF ) which has been placed in the receiver system(10).

First, a resolution phantom experiment was carried out by using the conventional gradient coil with the KAIST 2.0T whole-body MRI system. The result is shown in Fig.6(a). Next a high resolution image was obtained by using the new SGC set and the localized SE imaging sequence shown in Fig.4(a). The square region indicated in Fig.6(a) is the selected region for the localized high resolution imaging and Fig.6(b) is a simple zoomed image of the selected region of (a). Fig.6(c) is a high resolution image ( ~ $\Delta r$  = 50  $\mu$ m ) of the selected region obtained by using the SGC set. We have kept the same imaging parameters for all experiments ( Figs.6(a) and (c) ), i.e., repetition time ( T<sub>r</sub> = 500 msec. ), echo time ( T<sub>e</sub> = 30 msec. ), data acquisition time ( T<sub>acq</sub> = 5.12 msec. ) and

slice thickness ( 3 mm ) except the imaging time of each experiment. The imaging times of (a), (c) and (d) were 4.27 min., 12.8 min. and 30 min., respectively. Fig.6(c) clearly visualizes the fine structures of the resolution phantom with relatively good SNR compared with that of the conventional image ( Fig.6(a) ) despite of the resolution improvement of a factor of 20.

Fig.7 is a pair of a volunteer's knee image obtained using the conventional gradient and using the new SGC set. In these experiments, images are obtained by using SE imaging sequence with identical T<sub>r</sub> and T<sub>e</sub>. The localized high resolution images of an *in vivo* knee obtained by using the new SGC set visualizes many fine structures of the knee joint which were not previously seen by the conventional gradient system. It should be noted that the proposed new localized high resolution imaging using the SGC set does not require any major hardware modifications. In addition, we have experimentally observed that the SGC does not produce significant eddy current effects primarily due to the relatively long distance between the SGC and the inner bore of the magnet.

## Conclusions

In this paper we have described a new *in vivo* high resolution imaging scheme which is performed with a newly developed SGC set. The SGC set integrated with a surface RF coil proved to be an efficient *in vivo* high resolution imaging system and is especially useful for localized human body imaging which is not possible by use of the conventional gradient coil. The SGC described in this paper in conjunction with an integrated RF coil suggests the potential of the movable probe in the future such as the hand-held NMR imaging probe similar to the movable probe used in the ultrasound scanner.

## References

1. G.A.JOHNSON, M.B. THOMPSON, S.L. GEWALT AND C.E.HAYES, *J. Magn. Reson.*, **68**, 129 (1986).
2. C.D.ELLES AND P.T. CALLAGHAN, *J. Magn. Reson.*, **68**, 393 (1986).
3. Z.H. CHO, C.B. AHN, S.C. JUH, H.K. LEE, R.E. JACOBS, S. LEE, J.H. YI AND J.M. JO, *Med. Phys.*, **15**, 815 (1988).
4. G.P.COOPER, J.M.BROWN AND G.A.JOHNSON, *J. Magn. Reson.*, **83**, 608 (1989).
5. *Magnetic Resonance Annual 1988*, Edited by H.Y.KRESSEL, Raven Press, New York (1988).
6. Z.H.CHO, H.S.KIM, H.B.HONG AND J.CUMMING, *Proceedings of the IEEE*, Vol.70, No.10, Oct., 1152 (1982).

7. P.MANSFIELD AND P.G.MORRIS, "NMR Imaging in Biomedicine.", Academic Press, New York (1982).
8. J.H. YI AND Z.H. CHO, *Abstr. Soc. Magn. Reson. Med.*, 201 (1990).
9. F. ROMEO AND D.I. HOULT, *Magn. Reson. Med.*, 1, 44 (1984).
10. J.M. JO AND Z.H. CHO, *Abstr. Soc. Magn. Reson. Med.*, 206 (1990).

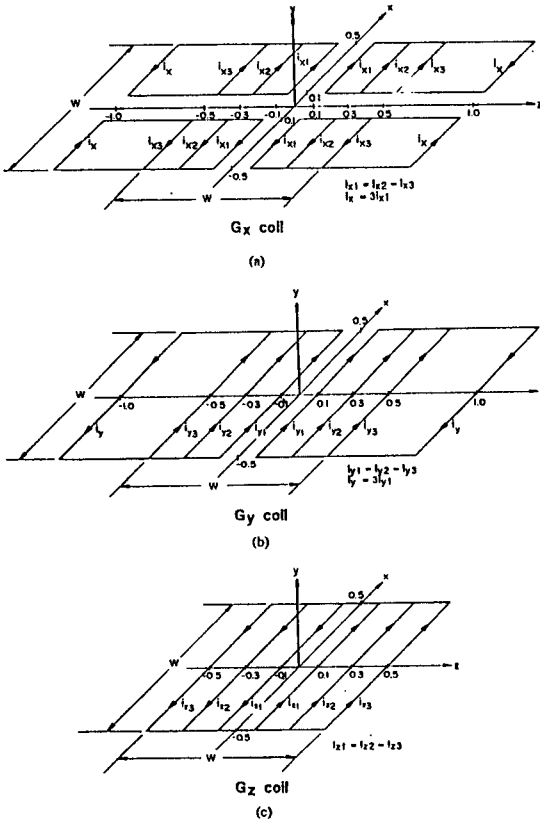


Fig. 1. Geometrical structures of the proposed surface gradient coil (SGC). (a)  $G_x$  coil, (b)  $G_y$  coil and (c)  $G_z$  coil. Note that the all dimensions are normalized by x-directional width ( $W$ ).

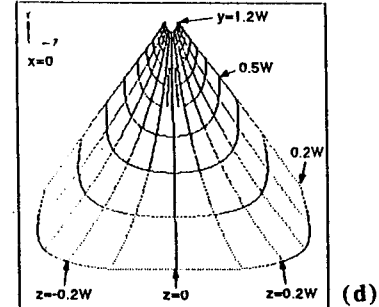
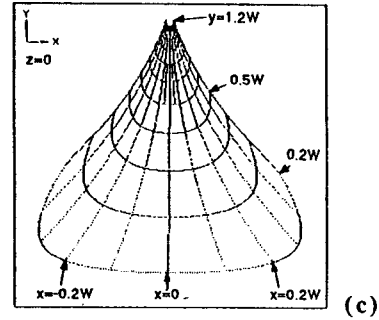
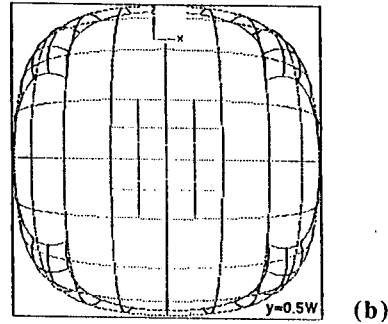
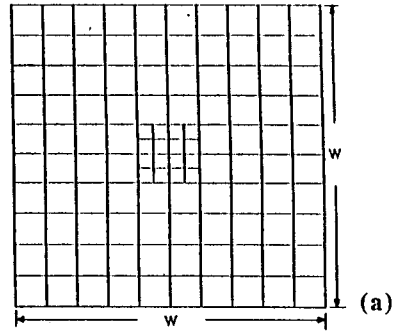


Fig. 2. Computer simulations of a 3-D grid phantom.

- (a) Cross section of the planar 3-D phantom used for the simulation, where a small high resolution structure of  $4 \times 4$  is embedded in the center.
- (b) Images of a parallel plane at different depths ( $y = 0.5W$ ).

- (c) An image of the plane parallel to the z-axis at  $z = 0$  where the planar phantom is placed parallel to the y-axis.
- (d) An image of the plane parallel to x-axis at  $x = 0$  where the planar phantom is placed parallel to the y-axis.

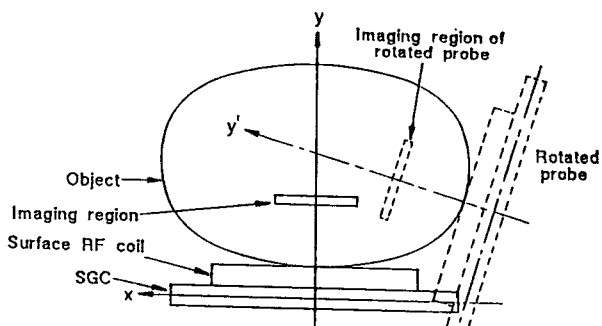


Fig. 3. An illustration of the movability of the SGC set (RF integrated). Region of any location parallel to the SGC set can be selected and imaged.

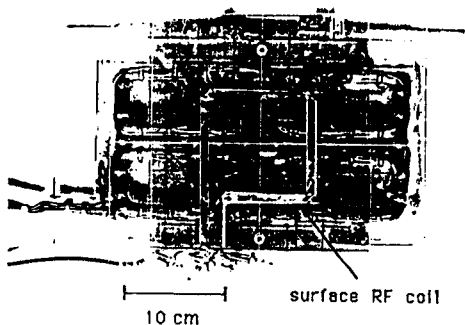


Fig. 5. Actual surface gradient coil constructed on a plane and combined with the surface RF coil.

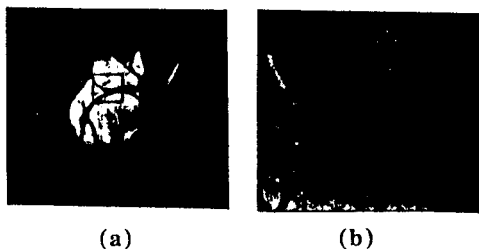


Fig. 7. Images obtained from a volunteer's knee.

(a) An image obtained by the conventional method using a surface RF coil. Slice thickness = 2 mm,  $T_R/T_E = 500/30$  msec., image matrix =  $256 \times 256$ ,  $T_{acq} = 5.12$  msec. and imaging time = 8.5 min.

(b) A high resolution image ( $\sim 100 \mu\text{m} \times 100 \mu\text{m}$ ) obtained by using the SGC set with the pulse sequence shown in Fig. 4(a). Imaging parameters; slice thickness = 2 mm,  $T_R/T_E = 500/30$  msec., image matrix =  $256 \times 256$ ,  $T_{acq} = 5.12$  msec. and imaging time = 51.2 min. Note here that the increased imaging time for the better SNR with high resolution image.

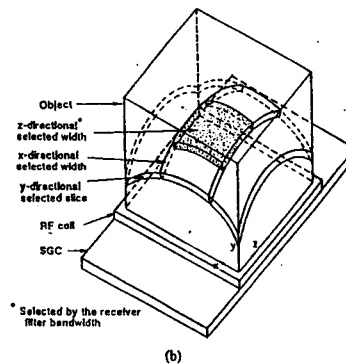
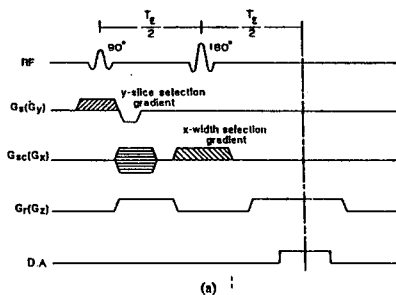


Fig. 4. A high resolution localized spin echo (SE) imaging pulse sequence and its imaging geometry. (a) Pulse sequence; a slice is first selected with  $G_S (=G_y)$  and a  $90^\circ$  RF pulse followed by the phase encoding in the z-direction by  $G_{SC} (=G_x)$ . Subsequent  $180^\circ$  RF pulse with a constant  $G_{sc} (=G_x)$  gradient following the coding  $G_{sc}$  selects the imaging region in the x-direction. Finally, the readout gradient  $G_r$  ( $G_z$ ) with a band-limited (low-pass) filter provides z-directional confinement of the selected region. (b) is the geometrical illustration of the above pulse sequence.

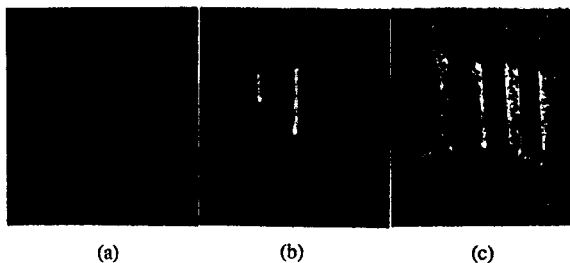


Fig. 6. (a) A water filled phantom image of a  $256 \times 256$  image matrix, approximately equivalent to a 1mm resolution obtained by the conventional gradient coil. (b) An image of the selected region of (a) zoomed by a factor of 20. (c) A high resolution ( $\sim 50 \mu\text{m} \times 50 \mu\text{m}$ ) image of the region of (a) obtained by using the SGC set and the pulse sequence shown in Fig. 4.